Published by :
http://www.ijert.org

International Journal of Engineering Research & Technology (IJERT)
ISSN: 2278-0181
Vol. 10 Issue 09, September-2021

River Network Classification from Multi-Spatial Satellite Imagery using Random Forest

Zeba Naaz
Department of Computer Science and Engineering
G. Narayanamma Institute of Technology & Science
Hyderabad, Telangana, India

Dr. G. Malini Devi
Department of Computer Science and Engineering
G. Narayanamma Institute of Technology & Science
Hyderabad, Telangana, India

***Abstract* - In recent years, the data science and remote sensing communities have started to align due to user-friendly programming tools, access to high-end consumer computing power, and the availability of high-resolution satellite data. Water-body segmentation is an important issue in remote sensing and image interpretation. Classic methods for counteracting this problem usually include the construction of index features by combining different spectra. However, these methods are essentially rule-based and fail to take advantage of context information. This paper presents a new framework for the segmentation of high-resolution hyperspatial data into river and non-river segments. This multi-step framework inculcates selection of feature extractors such as Gabor filter and canny edge detectors and implementation of Random Forest classifier algorithm for the segmentation task. The features extracted for each pixel encode quintessential contextual information and are compared with the precise annotated pixel information for classification. Finally, the random forest classification is carried out based on the pixel information for segmenting the high-resolution imagery into meaningful segmented maps classifying the river segments and non-river segments accurately. The proposed method, was applied to the hyperspatial satellite images. The experimental results show that the proposed method is more consistent for river mapping when compared to the predecessor methodologies. The overall pixel accuracy, IOU score, kappa statistics, F1 score, precision and recall obtained by the proposed method was 92.98%, 82.25%, 0.8474, 0.9026, 87.70% and 92.98%, respectively. Moreover, this method showed better efficiency in comparison to the spectral-based classifications.**

Keywords—Remote sensing, satellite imagery, river body segmentation, semantic segmentation, random forest.

I. INTRODUCTION

Water is one of the most important sources of life on Earth, and it is constantly changing. Waves pound the coast, causing erosion, river banks to be transformed by the flow of water, 3 glaciers to melt, resulting in new lakes and wetlands, reservoirs and harbors to be built, and much more. Accurate estimation of surface water changes is critical for a better understanding and management of the natural and anthropogenic processes that cause them. For decades, satellites were used to collect massive amounts of data, resulting in multi-petabyte archives of images collected. However, it has only been in the last decade, thanks to recent advances in cloud computing, that these massive amounts of data have been transformed into valuable knowledge. Segmentation is a process that assigns a predefined class nomenclature to every pixel in a raw image. Automatic segmentation is a fundamental feature in remote sensing and image interpretation, with water-body extraction being a typical application of this process. The primary distinction between image segmentation and semantic segmentation is that semantic segmentation attempts to create semantically meaningful regions [10]. Surface water detection methods that are accurate, efficient, and high-resolution are required for better water management. Surface water extent and dynamics datasets are critical for a better understanding of natural and man-made processes, as well as input data for hydrological and hydraulic models.

A. River monitoring

River monitoring is critical for providing flood protection, a sufficient amount of available water, and safe navigation for ships. Rivers are dynamic inland aquatic media that regulate and maintain a balanced adaptive community of organisms with a diverse species composition and functional organization in order to sustain a unique biotic integrity. Rivers provide a wide range of values and uses, including ecological stability, maintaining equilibrium, and direct-indirect production values.

B. Remote sensing

High-resolution satellite images are regarded as an essential source of information for resolving geographical issues such as socioeconomic issues in a variety of modern fields of study. These images, in conjunction with remote sensing techniques, help in a variety of domains. Remote sensing technology is used in a variety of applications, including land use land cover mapping, crop monitoring, change in land use detection, disaster management, and natural disaster analysis. Remote sensing (RS) in general, and Earth observation (EO) in particular, is a rapidly expanding field. One of the primary goals of this study was to create a set of fully automated algorithms and software tools for processing multi-spatial satellite imagery for surface water detection at high spatial resolutions.

II. RELATED WORK

Remote sensing technology enables effective surface water dynamics observation and continuous monitoring of the Earth's surface at multiple scales. Surface water detection based on water indices has been extensively researched in recent decades, and its ability to separate water from background features (non-water) has proven to be effective to some extent. Existing methods for detecting surface water from multispectral satellite data are based on the fact that

(This work is licensed under a Creative Commons Attribution 4.0 International License.)

International Journal of Engineering Research & Technology (IJERT)
ISSN: 2278-0181
Vol. 10 Issue 09, September-2021

water absorbs the vast majority of radiation at near-infrared and beyond wavelengths. Although more water indices for detecting surface water have recently been introduced, such as the Automated Water Extraction Index (AWEI) and Water Index (WI2015) no index has been proven to perform the best across all water and non-water pixel types using Landsat's resolution imagery [1, 2 & 3]. The researcher's contribution demonstrated that automatic feature extraction algorithms using Canny edge detector and Levenberg Marquardt methods are effective and accurate in extracting coastlines from satellite imagery [8]. The locally adaptive thresholding algorithm was used to segment images, these segmentation algorithms help by dividing the image into water and land areas. River boundaries were delineated using the SVM method from satellite images. They obtained an equivalent result using traditional methods, but was not effective enough to apply in real world applications [12].

For optical images, the researchers used a spectral matching method to investigate the likelihood of Landsat pixels being water bodies, and then used a particle swarm optimization method to achieve the best interpretation of water bodies [7]. This same contribution of automatic feature extraction techniques is also tested on road networks in Beirut, Lebanon, first by enhancing the satellite image, then segmenting the enhanced image, and finally applying morphological operators[11]. Similarly, for the purpose of extracting road networks from fused images of QuickBird, WorldView 2, and IKONOS 18 images, object-oriented segmentation was used, followed by a soft fuzzy classifier and morphological operators [9].

The researcher extracted farmland boundaries from grey scale HRSI using image processing algorithms. The work made use of canny edge detection, morphological operators, the Hough transform, and the discrete wavelet transform. They discovered that while some boundaries are not detected by the algorithms [15]. To construct semantic segmentation on magnetic resonance imaging (MRI) of brains, the researchers employed a Hidden Markov Random Field paired with their expectation-maximization approach. The authors do not present any segmentation challenge results and instead describe the problems in selecting basic tissue characteristics and classification [17].

VGG16 was utilized as the core network, and FCN models with three different up-sampling structures were built to extract multiscale water bodies [16]. The author presented a strategy integrating FCN with the GEE platform for off-line learning and online prediction to expedite extraction in urban river basins. The approach was validated in 36 urban regions across the country, with the F1 score and Kappa statistics of the majority of urban extraction findings reaching 0.9 [18].

The majority of the traditional water detection methods mentioned above are based on the use of spectral water indices, or possibly a supervised binary classification, in which images are classified into water and non-water classes. Even though recently developed methods provide better classification accuracy, they typically necessitate manual threshold adjustment to achieve the best results. As a result, their applicability to global studies while maintaining high accuracy is limited.

III.METHODOLOGY

In this section, the methodology is explained in detail of the proposed river network extraction for water-body segmentation from multi-spatial satellite Imagery shown in the figure 3.1. The methodology involved in the proposed framework are dataset collection, data preprocessing, feature extraction, training and testing the random forest model and finally assessment of the accuracy.

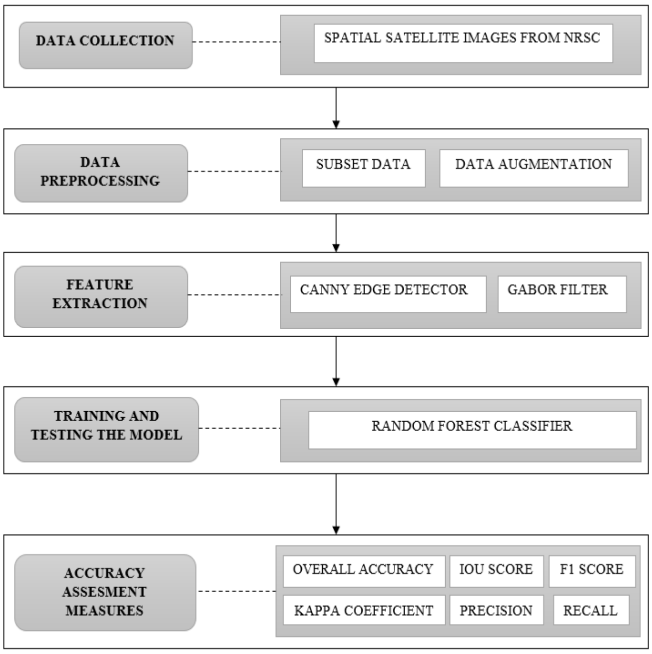

Fig 3.1: Methodology of the proposed system

A. Data collection

The remote sensing satellite imagery is collected from the satellites deployed by ISRO from the NRSC. For this project, Cartosat satellite mosaic data covering the area of interest that is, of a water body area near Andhra Pradesh, India was used for this project. The data is a mosaic of land area near Andhra Pradesh and is of size of 24GB.

B.Data preprocessing

This data needs to be preprocessed to obtain smaller subset images of dimension 512x512 which is done using Erdas imagine software [4]. Then annotation is performed to get labelled images which is achieved using apeer annotate tool [6] and viewed using ImageJ [5] . To obtain a more reliable dataset augmentation is performed on the dataset. Finally ,the dataset used to train the model consists of 4960 RGB images of 512x512 dimension which occupied 3.48GB on the system disk. Therefore approximately 1,300,234,240 pixels were used to model the proposed system in this project.

C.Feature extraction

Various feature extraction methods, such as canny edge detectors and gabor filters, are used to extract appropriate features from multi-spatial satellite images. Various authors compared the edge detection algorithms such as Canny,

(This work is licensed under a Creative Commons Attribution 4.0 International License.)

International Journal of Engineering Research & Technology (IJERT)
ISSN: 2278-0181
Vol. 10 Issue 09, September-2021

Sobel, Laplacian, and Zero Crossing and concluded that Canny's algorithm is best suited for feature extraction. Unlike other algorithms, Canny algorithms distinguished more features. It was also stated that the reason for its effectiveness in most contexts is that it produces fewer false edges [13].Many researchers have concluded that Canny's algorithm is the best detector in comparison to others. As a result, this algorithm has been chosen to be tested in the study [14].

D.Trainig and testing the model

The model for the classification of the river networks is then trained using the random forest classifiers. The model was trained with various train and test splits and on various user defined hyperparameters to obtain the model which outputs clear segmented maps of river and non-river water bodies.

E.Random forest classifier

Random forest classifiers are made up of a large number of classification and regression trees. The architecture of the random forest classifier is shown in the figure 3.2. The training data for each decision tree is bootstrap sampled from the entire data set, and the training data for each node in a decision tree is sampled without replacement from the entire data set. This bootstrap sampling strategy aids in the suppression of overfitting. Following the training of all decision trees, each produces a classification label and a vote for the final label, which is determined by majority voting. Because decision trees are trained in parallel, this procedure improves random forest robustness while decreasing running time.

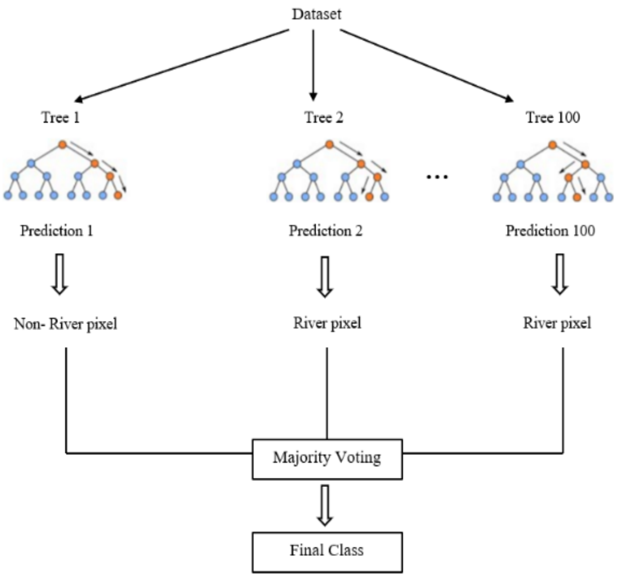

Fig 3.2: Architecture of the random forest classifier

F.Accuracy assessment

The accuracy of the model is then evaluated using the overall accuracy, IOU score, kappa coefficient, F1 score, precision and recall. Then performance of the random forest classifiers and the UNET model are then compared. Finally, a graphical user interface is developed for automatic extraction of river bodies based on the model which provided the best accuracy.

IV. IMPLEMENTATION

This project made use of Cartosat satellite mosaic data covering the area of interest, which was a water body area near Andhra Pradesh, India. The dataset used to train the model consists of 4960 512x512 images that took up 3.48GB on the system disc. The sample images and its respective masks are shown in the image 4.1. Out of which 4950 images were used to train and test the model and 10 images were used to segment the satellite map into river body and non-river body. As a result, roughly 1,300,234,240 pixels were used in this project. The segmentation problem entailed categorizing land cover as water or non-water. Satellite imagery images are trained using labelled data, and feature extraction is carried out using various filters such as the Gabor filter and canny edge detector.

Satellite imagery has a wide range of texture types that represent various target areas such as roads, rivers, lakes, land, vegetation, buildings, and more. Many applications for sustainable project management seek to distinguish these areas in grayscale and/or color images, and edge detection has been used as the feature extraction step prior to the other subsequent stages of data processing. Edges detect and localize significant changes in a digital image. These variations could be caused by object boundaries, textural properties, or illumination. The Gabor filter is a linear filer that is used in image processing applications such as edge detection, texture analysis, and feature extraction. This filter has been shown to have optimal localization, particularly in the spatial domain, and is thus well suited for texture segmentation problems.

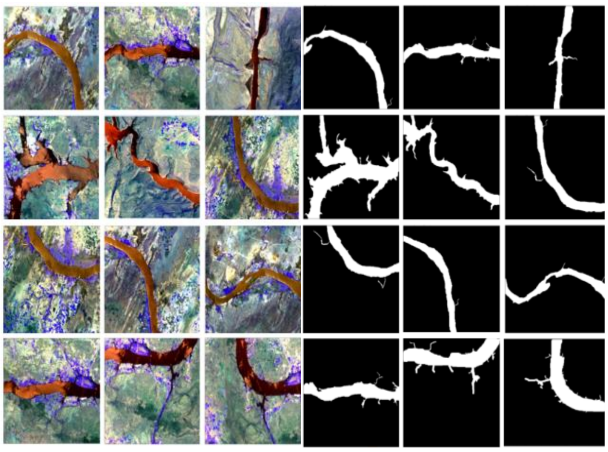

Fig 4.1: Sample images and masks

The segmentation problem entailed categorizing land cover as water or non-water. Satellite imagery images are trained using labelled data, and feature extraction is carried out using various filters such as the Gabor filter and canny edge detector. Satellite imagery has a wide range of texture types that represent various target areas such as roads, rivers, lakes, land, vegetation, buildings, and more. Many applications for sustainable project management seek to distinguish these areas in grayscale and/or color images, and edge detection has been used as the feature extraction step

(This work is licensed under a Creative Commons Attribution 4.0 International License.)

International Journal of Engineering Research & Technology (IJERT)
ISSN: 2278-0181
Vol. 10 Issue 09, September-2021

prior to the other subsequent stages of data processing. Edges detect and localize significant changes in a digital image. These variations could be caused by object boundaries, textural properties, or illumination. The Gabor filter is a linear filer that is used in image processing applications such as edge detection, texture analysis, and feature extraction. This filter has been shown to have optimal localization, particularly in the spatial domain, and is thus well suited for texture segmentation problems.

The main challenge in detecting rivers from remotely sensed imagery is that thin rivers frequently have low spatial contrast with the image background. The architecture of the proposed system is shown in the figure 4.2.

The Canny algorithm has been improved in terms of noisy edges. To reduce the noise effect, the image is smoothed using a Gaussian filter. The intensity gradients are then computed to determine the edge strength and direction, as in other gradient-based edge detection algorithms. Edge pixels that exceed the high threshold are labelled as strong edges, while those that fall below the low threshold are discarded, and pixels that fall between the two thresholds are labelled as weak edges.

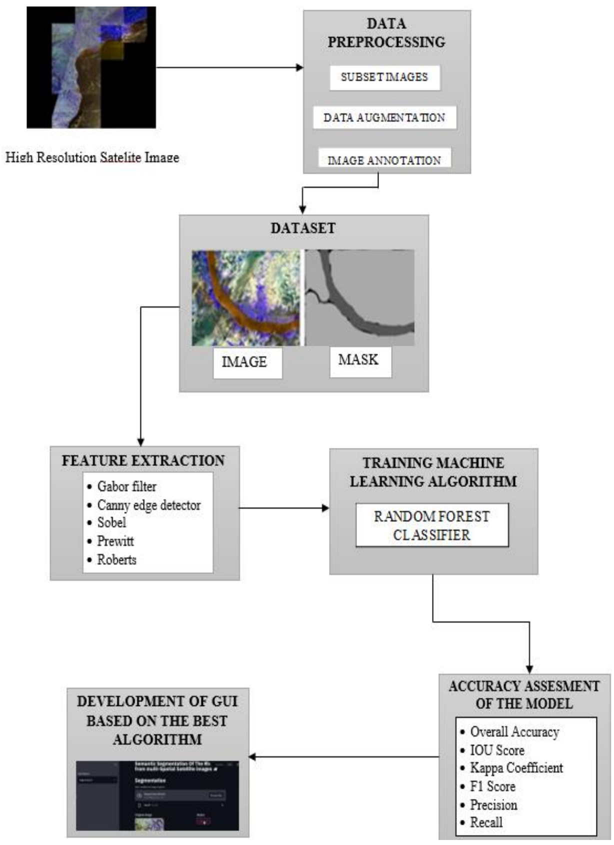

Fig 4.2: Architecture of the proposed system

Several random forest model implementations were carried out in order to select the user-defined parameters for the random forest classifier that outperformed other models. The random forest parameters were set to various numbers of estimators such as 10, 30, 50, 70, 100, and 150 across various training and test splits for this implementation. The effectiveness of the segmentation is evaluated using measures such as pixel accuracy, intersection over union (IOU) score, kappa coefficient, F1 score, precision and recall.

V. EVALUATION METRICS

Performance indicators for classification problems include comparing the expected class label to the predicted class label or interpreting the predicted probabilities for the problem's class labels. In this project, overall accuracy, IOU Score, kappa coefficient F1- score, recall and precision were used to evaluate the model's performance.

A.Overall Accuracy

Accuracy is the percentage of image pixels that are correctly classified. It is also referred to as overall pixel accuracy. It is the most fundamental performance metric, but it has the limitation of misrepresenting image segmentation performance in the event of class imbalance.

$$\text{Accuracy} = \frac{\text{Correctly Predicted Pixels}}{\text{Total number of Image Pixels}} = \frac{TP + TN}{TP+TN+FP+FN} \quad (1)$$

Where TP, TN, FP and FN in equation 1 represents the true positive,true negative, false positive and false negative values.

B.IOU Score

The Jaccard similarity index, commonly known as the Intersection over Union (IoU) metric. It is defined as the ratio of the predicted segmentation's overlap with the ground truth segmentation to the predicted segmentation's union with the ground truth segmentation.

$$\text{IOU} = \frac{A \cap B}{A \cup B} = \frac{TP}{TP+FP+FN} \quad (2)$$

Where A and B in equation 2 represents ground truth pixels and predicted pixels respectively. The TP, TN, FP and FN values in equation 2 represent true positive, true negative, false positive and false negative pixel values respectively.

C.Kappa Coefficient

The Kappa coefficient is a statistic that compares observed and expected accuracy. Cohen's kappa is a statistical coefficient that indicates the degree of accuracy and reliability in a statistical classification.

$$K = \frac{Pr(a) - Pr(b)}{1 - Pr\ (b)} \quad (3)$$

Where Pr(a) is the model's overall accuracy and Pr(b) is the measure of agreement between model predictions and actual class values as if they happened by chance in equation 3.

D.Precision

Precision is defined as the proportion of relevant instances in the total number of retrieved instances. Precision is calculated by dividing the number of true positives by the number of true positives plus the number of false positives.

$$\text{Precision} = \frac{TP}{TP+FP} \quad (4)$$

(This work is licensed under a Creative Commons Attribution 4.0 International License.)

The TP and FP values in equation 4 represent true positive and false positive pixel values respectively.

E.Recall

The recall statistic is used to assess a model's ability to find all relevant cases within a dataset. The ability of a model to find all of the data points of interest in a dataset is referred to as recall.

$$\text{Recall} = \frac{TP}{TP+FN} \quad (5)$$

The TP and FN values in equation 5 represent true positive and false negative pixel values respectively.

F.F1 Score

The F1-score or F1-measure is a measure of a model's accuracy in binary classification statistical analysis. The F1 score is calculated by taking the harmonic mean of precision and recall. The Sørensen–Dice coefficient or Dice similarity coefficient (DSC) is another name for the F1 score.

$$\text{F1}= 2.\frac{\text{precision.recall}}{\text{precision+recall}} \quad (6)$$

VI. RESULTS AND DISCUSSION

Several random forest model implementations were carried out in order to select the user-defined parameters for the random forest classifier that outperformed other models. The random forest parameters were set to various numbers of estimators such as 10, 30, 50, 70, 100, and 150 across various train and test splits for this implementation.

The input satellite image segmentation has been performed with the random forest algorithm with various random forest parameters and the effectiveness of the segmentation is analyzed by the measures as Accuracy and Intersection over union (IOU) score as depicted in the table 5.1.

Table 5.1: Comparative analysis of the random forest model for various number of estimators and with train and test split ratio of 60-40% using overall accuracy and IOU score as evaluation metrics.

Random Forest Model	Number Of Estimators	Overall Accuracy	IOU Score
RF model-1	10	54.62%	47.21%
RF model-2	30	59.81%	52.67%
RF model-3	50	61.30%	55.62%
RF model-4	70	63.97%	57.43%
RF model-5	100	66.21%	60.66%
RF model-6	150	64.46%	58.54%

From the table 5.1 it is observed that the random forest model 5 performed the best with 100 number of estimators with 66.21% overall accuracy and IOU score of 60.66%.

Table 5.2: Comparative analysis of the random forest model for various number of estimators and with train and test split ratio of 70-30% using overall accuracy and IOU score as evaluation metrics.

Random Forest Model	Number Of Estimators	Overall Accuracy	IOU Score
RF model-7	10	88.31%	75.84%
RF model-8	30	88.49%	76.45%
RF model-9	50	89.31%	78.67%
RF model-10	70	90.78%	80.81%
RF model-11	100	92.98%	82.25%
RF model -12	150	91.95%	81.99%

Table 5.2 shows that the random forest model 11 performed the best with 100 estimators, achieving 92.98% overall accuracy and an IOU score of 83.17 %.

Table 5.3: Comparative analysis of the random forest model for various number of estimators and with train and test split ratio of 80-20% using overall accuracy and IOU score as evaluation metrics.

Random Forest Model	Number Of Estimators	Overall Accuracy	IOU Score
RF model-13	10	71.42%	65.69%
RF model-14	30	68.21%	63.55%
RF model-15	50	66.87%	62.76%
RF model-16	70	65.42%	61.68%
RF model-17	100	65.37%	59.32%
RF model-18	150	63.12%	58.65%

The random forest model 16 performed the best with 70 estimators, 65.42 % overall accuracy, and an IOU score of 61.68 %, as shown in table 5.3.

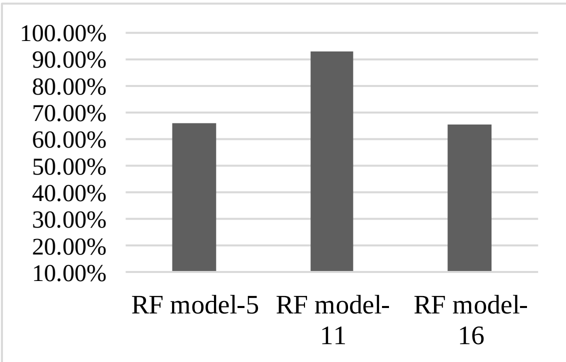

(a).

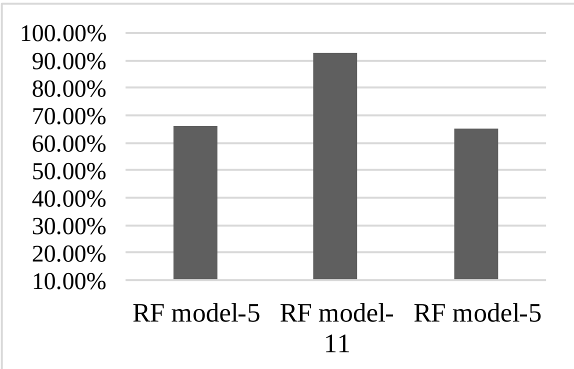

(b).

Fig 5.1 Comparative analysis of random forest models using (a) overall accuracy and (b)IOU score as the evaluation metric.

(This work is licensed under a Creative Commons Attribution 4.0 International License.)

International Journal of Engineering Research & Technology (IJERT)
ISSN: 2278-0181
Vol. 10 Issue 09, September-2021

From the figure 5.1 it is observed that the random forest model trained on 70% images and tested with the remaining 30 percent of the images with 100 number of estimators performed the best among all the random forest models. This model achieved overall accuracy score of 92.98% and IOU score of 83.17%.

Table 5.4: Accuracy assessment of the optimal random forest model and UNET model using overall accuracy, IOU score, kappa coefficient, F1 score, precision and recall as evaluation metrics

Model	OA	IOU Score	Kappa Coeff.	F1 Score	Precision	Recall
Random forest	92.98%	82.25%	0.84	0.9026	87.70%	92.98%

From the table 5.4 it is observed that the random forest model outperformed the predecessor models with the 92.98% overall accuracy. Also, random forest achieved higher IOU score, kappa coefficient, F1 score, recall and precision that is 82.25%, 0.8478, 0.9026, 87.70% and 92.98% respectively. which interprets as a very good agreement when compared to the metrics obtained by the existing system.

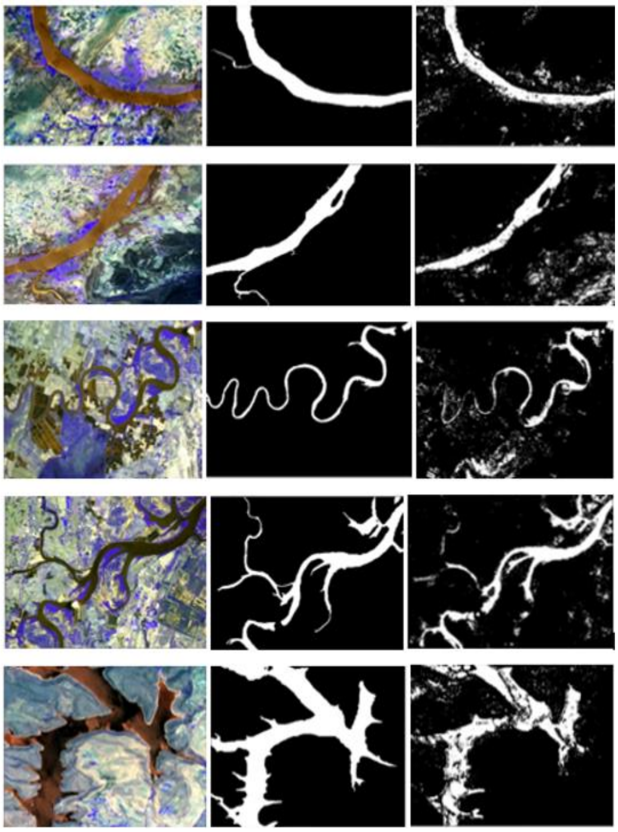

(a) (b) (c)

Fig 5.2: Comparative analysis of the segmented maps produced by random forest and ground truth. Figure (a) represents the original test image, figure (b) represents the ground truth and figure (c) represents the segmentation performed by the random forest model.

In the figure 5.2 it is observed that the random forest classifier produces the segmented maps of the satellite imagery. The random forest model produced minimum noise in the segmented map when compared to the existing models and could clearly identify the finer river bodies as well.

VII. CONCLUSION AND FUTURE WORK

Accurate estimation of these surface water changes is critical for improving understanding and management of the natural and anthropogenic processes that cause them. Traditional methods for mapping river water often produce significant uncertainties. The creation of an automated map of the presence or absence of various land covers will significantly reduce the burden on manual editing and checking in the pursuit of a high-quality map to support a variety of government policies.

A robust methodology for efficient and highly precise segmentation of surface river water and land is proposed. The proposed network achieves the goal of automatically extracting the water body from different images of the Cartosat satellite. The random forest model achieved 92.98%, 82.25%, 0.8474, 0.9026, 87.70% and 92.98% as overall accuracy, IOU score, kappa coefficient, F1 score, precision and recall respectively.

To meet the standards of surveying and mapping products, there is still a long way to go. In the current research field, determining how to make active intelligent extraction and vector map construction for complex scene water bodies covered by the entire space, and then continuously monitor and update with observation accumulation, will be more difficult. In terms of water resource management, this method can be extended to rapid data analysis of flooding and other thematic information.

REFERENCES

[1]. Adrian Fisher, Neil Flood, and Tim Danaher., "Comparing Landsat water index methods for automated water classification in eastern Australia.", Remote Sensing of Environment, vol. 175, pp. 167– 182, 2016.

[2]. Gudina L. Feyisa, Henrik Meilby, Rasmus Fensholt and Simon R. Proud., "Automated water extraction index: A new technique for surface water mapping using Landsat imagery.", Remote Sensing of Environment, vol. 140, pp. 23–35, 2014.

[3]. Guy J. P. Schumann and Delwyn K. Moller., "Microwave remote sensing of flood inundation.", Physics and Chemistry of the Earth, vols. 83–84, pp. 84-95, 2015.

[4]. https://erdas-imagine.software.informer.com/download/

[5]. https://imagej.nih.gov/ij/download.html

[6]. https://www.apeer.com/home

[7]. Kai Jia, Weiguo Jiang, Jing Li and Zhenghong Tang., "Spectral matching based on discrete particle swarm optimization: A new method for terrestrial water body extraction using multi-temporal Land sat 8 images.", Remote Sensing Environment, vol. 209, pp. 1–18, 2018.

[8]. Liu. H and Jezek K. C., "Automated extraction of coastline from satellite imagery by integrating Canny edge detection and locally adaptive thresholding methods.", International Journal of Remote Sensing, vol. 25, pp. 937–958, 2004.

[9]. M. Kumar, R. K. Singh, P. L. N. Raju, Y. V. N. Krishnamurth., "Road Network Extraction from High Resolution Multispectral Satellite Imagery Based on Object Oriented Techniques.", ISPRS Annals of Photogrammetry, Remote Sensing and Spatial Information Sciences, vol. 2, pp. 107–110, 2014.

(This work is licensed under a Creative Commons Attribution 4.0 International License.)

[10]. Martin Thoma., “A survey of semantic segmentation.” Computer Vision and Pattern Recognition, vol. 31, pp. 1-16, 2016.
[11]. Mohamad M. Awad., “A Morphological Model for Extracting Road Networks from High-Resolution Satellite Images.”, Journal of Engineering, vol. 2013, 1–9, 2013.
[12]. Paramate Horkaew, Supattra Puttinaovarat and Kanit Khaimook., “River boundary delineation from remote sensed imagery based on SVM and relaxation labeling of water index and DSM.”, Journal of Theoretical and Applied Information Technology, vol. 71, pp. 376–386, 2015.
[13]. S.K. Katiyar and P.V. Arun., “Comparative analysis of common edge detection techniques in context of object extraction.” , IEEE Transactions on Geoscience and Remote Sensing, vol. 50, pp. 68-79, 2014.
[14]. Shi Guiming and Suo Jidong., “Remote sensing image edge-detection based on improved Canny operator.”, 8th IEEE International Conference on Communication Software and Networks, vol. 67, pp. 652-656, 2016.
[15]. Usman Babawuro and Zou Beiji., “Satellite Imagery Cadastral Features Extractions using Image Processing Algorithms: A Viable Option for Cadastral Science.”, International Journal of Computer Science Issues, Vol. 9, pp. 30-38, 2012.
[16]. Wang Xue, Sui Lichun, Zhong Mianqing, Li Dingmeng and Dang Lili., “Fully convolution neural networks for water extraction of remote sensing images.”, Bulletin of Surveying and Mapping, vol. 6, pp. 41-45, 2018.
[17]. Yongyue Zhang, Michael Brady, and Stephen Smith., “Segmentation of brain MRI images through a hidden markov random field model and the expectation-maximization algorithm.”, IEEE Transactions on Medical Imaging, vol. 20, pp. 45–57, 2001.
[18]. Yudie Wang, Zhiwei Li, Chao Zeng , Gui-Song Xia , and Huanfeng Shen., “An urban water extraction method combining deep learning and google earth engine.”, IEEE Journal Of Selected Topics In Applied aEarth Observations And Remote Sensing, vol. 13, pp. 768-781, 2020.

(This work is licensed under a Creative Commons Attribution 4.0 International License.)